Plan Quality and Sensitivity Analysis of Conformal Arc Informed Volumetric Modulated Arc Therapy (CAVMAT)

by

Edward Thomas Cullom IV

Graduate Program in Medical Physics
Duke University

Date:_______________________
Approved:

____
Justus Adamson, Advisor

____
William Giles

____
Yunfeng Cui

____
Michael Moravan

This thesis is submitted in partial fulfillment of
the requirements for the degree of
Master of Science in the Medical Physics Graduate Program in Medical Physics
in the Graduate School of Duke University

2020

ABSTRACT

Plan Quality and Sensitivity Analysis of Conformal Arc Informed Volumetric Modulated Arc Therapy (CAVMAT)

by

Edward Thomas Cullom IV

Medical Physics Graduate Program
Duke University

Date:________________________
Approved:

____
Justus Adamson, Supervisor

____
William Giles

____
Yunfeng Cui

____
Michael Moravan

An abstract of a thesis submitted in partial
fulfillment of the requirements for the degree
of Master of Science in the Medical Physics Graduate Program in the Graduate School of
Duke University

2020

Abstract

Purpose: Linac based radiosurgery to multiple metastases is commonly planned with VMAT as it effectively achieves high conformality to complex target arrangements. However, as the number of targets increases, VMAT may struggle to block between targets, which may lead to highly modulated and/or nonconformal MLC trajectories. This phenomenon is particularly apparent in multi-target geometries as targets often share the same MLC leaf pair, creating an MLC opening and yielding insufficient inter-target collimation. Given the complex geometries, multi-target SRS necessitates high degrees of dosimetric accuracy. Dosimetric accuracy may be impacted by beam commissioning as a single dosimetric leaf gap (DLG) must be selected and used for all targets, geometries, and MLCs. Conformal Arc Informed VMAT (CAVMAT) aims to reduce healthy tissue dose by utilizing simplified MLC trajectories and by producing more conformal dose distributions. It is hypothesized that the simplified leaf motion and reduced complexity of CAVMAT may reduce sensitivity to commissioning and treatment delivery uncertainty.

Materials & Methods: CAVMAT is a hybrid treatment planning technique which combines the conformal MLC trajectories of dynamic conformal arcs with the MLC

modulation and versatility of inverse optimization. CAVMAT has three main steps. First, targets are assigned to subgroups to maximize MLC blocking between targets. Second, arc weights are optimized to achieve the desired target dose, while minimizing MU variation between arcs. Third, the optimized conformal arc plan serves as the starting point for limited inverse optimization to improve dose conformity to each target. Twenty multifocal VMAT cases were re-planned with CAVMAT with 20Gy applied to each target. The total volume receiving 2.5 Gy, 6 Gy, 12 Gy, and 16 Gy, conformity index, treatment delivery time, and the total MU were used to compare the VMAT and CAVMAT plans. Of the 20 VMAT plans, 10 were selected and replanned with CAVMAT, at DLG values of 0.4 mm, 0.8 mm, and 1.2 mm and the change in V_{6Gy}[cc], V_{12Gy}[cc], V_{16Gy}[cc], and target dose was quantified. The 10 VMAT and CAVMAT plans were delivered to a $Delta^4$ QA phantom and dose agreement was quantified using gamma index with 3%/1mm, 2%/1mm, and 1%/1mm criteria. Trajectory log files were collected and analyzed to quantify MLC positioning errors during delivery. 16 targets were selected, with at least one target from each plan, and were delivered to an SRS Mapcheck QA phantom to evaluate dose difference per DLG.

Results: After replanning the 20 VMAT cases, CAVMAT reduced the average $V_{2.5Gy}$[cc] by 25.25±19.23%, V_{6Gy}[cc] by 13.68±18.97%, V_{12Gy}[cc] by 11.40±19.44%, and V_{16Gy}[cc] by 6.38±19.11%. CAVMAT improved conformity by 3.81±7.57%, while maintaining comparable target dose. MU for the CAVMAT plans increased by 24.35±24.66%, leading to an increased treatment time of ~2 minutes. For the DLG analysis, the 10 VMAT plans demonstrated an average sensitivity to variation of V_{6Gy}[cc], V_{12Gy}[cc], V_{16Gy}[cc] of 35.83 ± 9.48 $\frac{\%}{mm}$, 34.12 ± 6.61 $\frac{\%}{mm}$, and 39.22 ± 8.41 $\frac{\%}{mm}$, respectively, compared to 23.18 ± 4.53 $\frac{\%}{mm}$, 22.45 ± 4.28 $\frac{\%}{mm}$, and 24.88 ± 4.91 $\frac{\%}{mm}$ for CAVMAT. VMAT was found to be roughly twice as sensitive as CAVMAT to changes in target doses for a varying DLG. For the plans delivered to the Delta^4 CAVMAT demonstrated an improved dose agreement, with the strictest criteria of 1%/1mm resulting in a passing rate of 94.53 ± 4.42% for VMAT compared to 99.28 ± 1.74% for CAVMAT. Log file analysis demonstrated CAVMAT's improved resistance to treatment delivery uncertainties, though the difference compared to VMAT is not expected to be substantial.

Conclusions: The CAVMAT technique successfully eliminated insufficient MLC blocking between targets prior to the inverse optimization, leading to less complex treatment plans and improved tissue sparing. CAVMAT is more robust to dosimetric and treatment delivery uncertainties and better maintains target dose and healthy tissue sparing. The reduced complexity, inherent tissue sparing, improved conformity, and reduced sensitivity to uncertainties indicates CAVMAT to be a promising method to treat brain metastases.

Contents

List of Tables

List of Figures

List of Abbreviations

CI – Conformity index

DCA – Dynamic conformal arcs

DLG – Dosimetric leaf gap

DVH – Dose volume histogram

MLC – Multi-leaf collimator

MU – Monitor unit

OAR – Organ at risk

SBRT – Stereotactic body radiation therapy

SIDCA – Single isocenter dynamic conformal arcs

SIMT – Single isocenter multiple targets

SRS – Stereotactic radiosurgery

TPS – Treatment planning system

VMAT – Volumetric modulated arc therapy

WBRT – Whole brain radiation therapy

Acknowledgements

I would first like to thank my advisor, Dr. Justus Adamson, for his support, encouragement, and patience. There was never a question too trivial and his door was never closed. Despite having multiple students and various different projects, each one of us received his wholehearted attention. I would also like to thank Dr. William Giles for his continual support and the many hours spent helping me over the last two years. Your expertise, willingness to help, and sense of humor made research a very productive and rewarding experience. The extra time spent during lunch breaks or after hours to help me tackle certain obstacles was greatly appreciated. I consider myself very fortunate to have worked with you both; I could not have chosen a better lab.

I would like to express my appreciation to Dr. Yunfeng Cui and Dr. Michael Moravan for their time and contributions to my thesis committee. Dr. Anna Rodrigues, your interest in education, student involvement, and willingness to teach were greatly appreciated. The completion of my thesis work would not have been possible without support and collaboration from my lab mates: Yuqing Xia and Kai-Cheng Chuang.

Thank you to my family for encouraging me to tinker with things from a young age; who knows where I would be without lincoln logs and legos. Lastly, thank you to Courtney Link for support, numerous flights, and for forcing me away from work.

1. Introduction

1.1 Stereotactic radiosurgery for brain metastases

Brain metastases are conservatively estimated to occur in 9-17% of all cancer patients, with some studies reporting higher incidence rates of 20 - 40%[1-2]. Historically, WBRT was utilized for patients with multiple brain metastases, patients who were not candidates for surgical resection, or as adjuvant therapy in patients with a single brain metastasis undergoing surgical resection to reduce the rates of CNS recurrence and neurologic death [3]. WBRT is a palliative treatment and only temporarily halts the growth of brain metastases, gradually reducing any associated mass effect and subsequent neurologic symptoms. The most common WBRT is 30 Gy delivered over 10 daily fractions, though numerous dose/fractionation schemes exist [4].

Stereotactic radiosurgery (SRS) utilizes steep dose gradients and high degrees of accuracy to treat brain metastases in one to five fraction. Combining SRS and WBRT improves local control rates but did not improve overall survival to WBRT alone [5]. Patients receiving SRS and WBRT, however, experienced decreased quality of life compared to patients treated with SRS alone, with long-term survivors demonstrating a greater incidence of cognitive deterioration at 3 and 12 months [6,7]. Additionally, a prospective, observational, and non-inferiority study enrolled newly diagnosed, good performance status patients with 1-10 brain metastases receiving SRS to all intracranial disease and demonstrated non-inferior median overall survival for patients with 5-10 brain metastases versus those with 2-4 brain metastases, with no difference in the rate of treatment-related adverse events [8]. Because of these findings, SRS has largely replaced WBRT in the treatment of patients with a limited number of metastatic brain lesions.

1.2 Dynamic Conformal Arcs

Conventional linear accelerator-based SRS can be performed using several different techniques. Dynamic conformal arc (DCA) radiation therapy can be used to deliver SRS to treat brain metastases. DCA techniques dynamically conform the multi-leaf collimator (MLC) to the targets in question throughout the gantry rotation. In treatment scenarios involving multiple targets, each target is assigned its own isocenter and is treated sequentially. DCA radiation therapy often results in extended patient set-up and total treatment times, particularly when differing couch angles are utilized. Single isocenter dynamic conformal arc (SIDCA) treatment techniques allow for targets to be treated simultaneously, substantially reducing the required treatment time [9,10]. The MLCs in a SIDCA treatment conform to each target, or a select group of targets, for a given arc. This allows for conformal MLC trajectories that sufficiently block between targets and prevent unnecessary MLC openings. While SIDCA is highly conformal, the technique is limited in flexibility. SIDCA seeks to conform the MLCs closely to each target, which can be difficult when treating targets that are irregular in shape or close in proximity to critical structures.

1.3 Volumetric Modulated Arc Therapy

Volumetric Modulated Arc Therapy (VMAT) is a highly flexible radiotherapy technique that can also utilize a single isocenter for quick and effective multi-target radiosurgery [11]. VMAT includes an inverse optimization component, which allows for more flexibility to meet unique plan-specific constraints, such as conforming dose to irregular shaped targets or minimizing dose to proximal OARs [9]. Single isocenter radiosurgery has grown in popularity, with many recent advancements in SIMT VMAT radiosurgery such as advanced treatment planning techniques [11-15], physics considerations and quality assurance aspects related to treatment [16-20,35], and data relating to patient outcomes [21-23]. A reoccurring challenge of SIMT VMAT techniques is the inability of a single leaf pair to effectively collimate between multiple targets simultaneously, as seen in Figure 1. This dilemma was first highlighted by Kang, et al.; in their work they developed a method to help mitigate this collimation challenge by determining optimal collimator angles for each VMAT arc [26]. More recently Wu et al. developed an optimization algorithm to identify arc geometry (couch, collimator, and gantry) for VMAT with the least total unblocked are per arc [27]. While both approaches can help to reduce beam collimation challenges, in many instances targets overlapping with the same leaf pair cannot be avoided, a phenomenon that becomes increasingly problematic as the total number of targets increases. When target overlapping occurs, planners must manage the resulting tradeoffs between plan modulation and complexity, target coverage, and dose to normal tissue. Often the resulting inverse optimized VMAT plan will require fast moving and highly modulated MLC trajectories to achieve the desired dose distribution.

Previous studies have demonstrated that highly modulated and quickly changing MLC trajectories may decrease the dosimetric accuracy and effectiveness of a treatment plan [24,25]. As seen below in Figure 1, VMAT treatment plans involving multiple targets may position the MLCs such that leaf pairs completely obscure a target or fail to block between targets, creating MLC openings. When several targets share the same leaf pair VMAT may fail to block between targets, rendering the treatment planning system incapable of properly blocking healthy tissue at some gantry angles [26]. In this example targets 1, 3, and 6 are partially blocked, target 2 is completely obscured, and several openings are created on and around the targets.

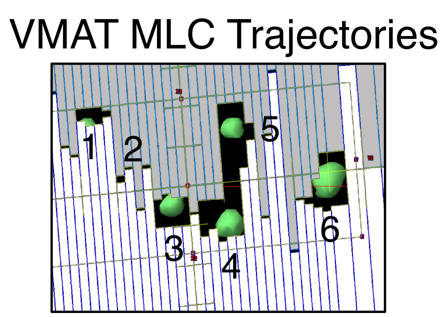

Figure 1: VMAT irregular MLC trajectories blocking targets and creating MLC openings

The irregular and unintended MLC openings often result in irregular-shaped dose distributions, dose bridging between targets, and an increased, unnecessary dose to healthy brain tissue. An example case demonstrating the irregular dose distributions and unnecessary dose bridging in multi-target VMAT plans is displayed below in Figure 2.

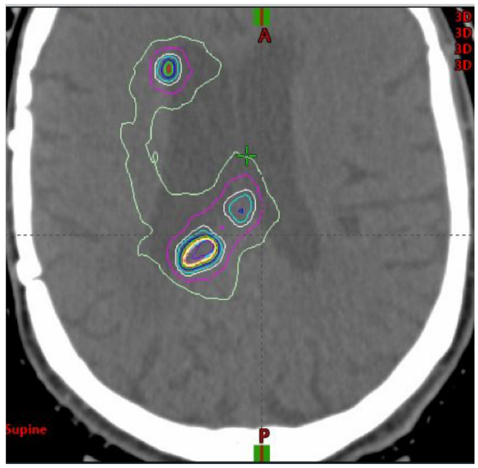

Figure 2: Irregular dose distribution and dose bridging in VMAT multi-target plan

Previous studies have investigated the use of optimized planning strategies to reduce the effect of insufficient MLC blocking between targets. These methods were found to be partially effective and highly dependent on specific treatment geometries [27,28]. Alternatively, inverse optimization can be used to reduce dose bridging between targets through contouring avoidance structures in the treatment planning system. The treatment planning system will attempt to limit the dose to the avoidance structure and will further constrain the MLC trajectories to minimize dose bridging. This technique is often inconsistent, time consuming, and may still result in complex MLC trajectories while only partially alleviating dose bridging. Aside from technique-specific limitations, there are limitations inherent to SRS that must be considered.

1.4 Challenges of small field dosimetry

The success of external beam radiation therapy is largely dependent on accurate modeling of the photon beam in the treatment planning system [29]. Photon beam models are built using commissioned beam data, which is subject to error from the detector, the phantom, and the treatment machine that was used for data collection [30]. The difficulty of accurate beam modeling is exacerbated when small radiation fields are used.

The use of small radiation fields, as is common in SRS and SBRT applications, introduces several complications that are not present when larger fields are utilized. A small radiation field can be defined as a field size which is smaller than the lateral range of charged particles created along the central beam axis. This can further be described as a field size for which lateral charged particle equilibrium fails. For a 6 MV photon beam field sizes smaller than $3\ x\ 3\ cm^2$ are considered to be small radiation fields [31]. The loss of charged particle equilibrium paired with steep dose gradients complicates dosimetric measurements and the accurate modeling of small fields.

SRS techniques commonly employ substantial collimation, which can obscure the primary beam if small fields are used. If the primary beam is substantially blocked, the beam penumbras may overlap resulting in a sizable reduction in beam output [32-34]. Given that the use of small fields increases the potential for error or exacerbate existing error, it is crucial to investigate a treatment technique's sensitivity and resistance to various sources of uncertainty.

1.5 TPS Modeling Uncertainty

In Varian systems, the dosimetric leaf gap (DLG) can have substantial dosimetric impact, particularly for highly modulated fields that are typical for multi-target VMAT. Varian HD-MLC systems feature rounded MLC leaves, as opposed to fully rectangular leaves, in order to maintain a relatively constant penumbra at varying field sizes [35]. While beneficial, the rounded leaf ends create a discrepancy between the geometric and dosimetric field widths due to transmission through the rounded edges [36]. The dosimetric leaf gap (DLG) is a commissioned parameter which models the physical difference between the linear accelerator light and radiation fields and attempts to account for transmission through the rounded leaf ends. The DLG is effectively a parameter which determines the modeled distance between MLC leaves, when they are set to be completely closed and abutting. The specific DLG value can be optimized such that measured dose distributions for a set of plans match the treatment planning system calculations [36].

For a given beam model, the optimal DLG value will likely differ depending on the specific treatment plan and treatment site [37]. Given the unique treatment geometry inherent to multi-target radiosurgery, a degree of variation in the optimal DLG value is expected. Some institutional studies have reported difficulty in determining a single, optimal DLG value that is representative of all radiosurgery targets in a plan. In such scenarios it was necessary to divide the targets into multiple isocenter groups, partially negating the time-saving benefit of SIMT techniques [38,39]. While uncertainty is present in the DLG and beam modeling, it is also present in the treatment delivery itself.

1.6 Treatment Delivery Uncertainty

While optimal treatment plans and MLC patterns can be created in the treatment planning system, there are several physical parameters that may deviate from the expected performance when the plans are delivered. Upon treatment delivery, the physical motion of a given MLC leaf pair may deviate from the intended motion established in the treatment planning system. Similar deviations may occur in the gantry angle during the delivery of a treatment arc. SIMT radiosurgery techniques have been shown to be uniquely susceptible to treatment delivery uncertainties, particularly when targets are small and distant from the treatment isocenter [40-42]. Delivery uncertainties may be challenging to account for as there are few QA tools with sufficient resolution and dosimetric capacity to quantify the full effect. Current QA tools include various dosimeters and phantoms, as well as more fundamental techniques such as film analysis. While phantoms and detectors are effective, consideration must be given to the device's spatial resolution, as well as any angular dependences that may exist. Film analysis may be used but is often cumbersome and error prone as great care must be taken to accurately determine a dosimetric measurement. Similar to some phantoms, film is limited in applicable treatment angles. Log file analysis can subvert the resolution dilemma issue of most phantoms, as information is exported directly from the linear accelerator and may better highlight the physical motion of the MLCs.

1.7 Motivation

Conformal Arc Informed Volumetric Modulated Arc Therapy (CAVMAT) is a hybrid treatment planning technique currently under development which aims to overcome the physical and dosimetric limitations of VMAT for SIMT SRS applications. Specifically, CAVMAT can potentially overcome VMAT's insufficient MLC blocking between targets as well as reduce dose bridging between targets, while remaining robust to TPS modeling and treatment delivery uncertainties.

CAVMAT is designed to pair SIDCA and SIMT VMAT techniques, in which conformal MLC trajectories are used as the starting point for limited inverse optimization. CAVMAT aims to utilize the improved conformity and flexibility of MLC modulation inherent to inverse optimized VMAT, while producing more conformal MLC trajectories similar to SIDCA. These trajectories are capable of eliminating insufficient MLC blocking between targets, thus reducing healthy brain dose.

The CAVMAT treatment planning technique was refined and is composed of the following three main steps: target subgrouping, field weight optimization, and limited inverse optimization. The technique creates sets of conformal arcs that sufficiently collimate between targets and avoid dose bridging. The conformal arcs are assigned optimal field weights and limited inverse optimization is performed to increase dose conformity of each target.

2. Materials and Methods

2.1 Target Subgrouping

The CAVMAT technique may be applied to an arrangement of treatment arcs and target geometry that is judged to be acceptable for SIMT SRS. For each gantry and couch angle, all targets are divided into subgroups to be treated separately, with each group containing as many targets as the criteria below permits. Each target subgroup is assigned a copy of the arc, to be treated separately.

For the first subgroup of an arc, the first target may be selected at random. The addition of subsequent targets to a given subgroup is performed by prioritizing the following criteria, in order of importance: (1) a collimator angle can be found to allow complete collimation between the targets of a subgroup, (2) target superposition along the beam's eye view is not present, (3) the difference in the effective depth of targets in a subgroup is less than 5cm, (4) when the preceding criteria have been met, unique subgroups across all arcs may also be prioritized. Criteria (1) and (2) work in conjunction to limit dose bridging between targets [26]. Criterion (3) works to minimize dose differences between targets, which may be difficult to account for in the field weight optimization stage, as each arc will be assigned a constant MU per control point. Subgroup uniqueness is prioritized in criterion (4), as this may bolster the effectiveness of the subsequent field weight optimization, allowing it to better apply a uniform MU to each arc to achieve the desired dose, prior to the inverse optimization stage. The adjustment of the collimator angle and selection of target subgroups is an iterative process, often requiring the groups to be changed in order to find the optimal subgroup arrangement.

The subgrouping process is repeated for each arc in plan such that each arc is assigned a unique set of subgroups. The number of subgroups for each arc is largely dependent on the number of targets and the specific target geometry. More subgroups may be required in instances of complex target geometry, target superposition, or when a large number of targets are to be treated. For most treatment scenarios 2 subgroups for each base arc is sufficient.

Once all subgroups of an arc are finalized, each subgroup is assigned an identical copy of the arc in question, without changing the couch or gantry configuration. For a plan with 4 couch angles and an arc at each angle, 2 subgroups will be assigned to each arc, resulting in a plan with 8 total arcs but only 4 couch angles. To increase delivery efficiency the gantry motion for an arc may be reversed (i.e. clockwise for the first subgroup and counterclockwise for the second).

2.2 Creation of DCA plan

Following subgroup finalization, the MLCs for each arc were fit to a 1mm margin and the jaws were set to a 3 mm margin around the subgroup of the arc in question. This employs the intuitive and conformal MLC motions of a DCA plan and serves as the base for a CAVMAT plan.

2.2.1 MLC and Jaw Configuration

Initially a uniform 1 mm MLC and 1 mm jaw margin were used for the CAVMAT plans, but it was observed that the inverse optimization often prevented some MLC leaf pairs from fully extending to the jaw field size. This phenomenon was particularly apparent in situations involving small field sizes and small targets, resulting in static leaf pairs and target undercoverage. In a preliminary study, the 20 VMAT plans were replanned with the CAVMAT process with 3 different combinations of MLC and jaw margins. A uniform MLC and jaw margin of 2 mm and 1 mm were evaluated. A MLC margin of 1 mm was paired with a 3 mm jaw margin to attempt to mitigate the effect of static leaf pairs. The V_{6Gy}[cc], V_{12Gy}[cc], and V_{16Gy}[cc], total MU, and conformity index were evaluated to justify the selection of MLC and jaw settings. A jaw setting of 3 mm and MLC margin of 1 mm was found to adequately conform to the targets while maintaining a large enough field size to prevent target undercoverage and static leaf pair issues. The results of the preliminary investigation can be found in section 3.2.1. Jaw tracking was not used in the implementation and testing of the CAVMAT technique.

2.3 Field Weight Optimization

Following subgroup assignment and DCA creation, dose was calculated with a fixed MU for each field to provide an initial starting point for field weight optimization. Dose was normalized to 99.5% of the total PTV volume. Point doses from the center of each target were collected in order to determine the dose contribution for a uniform MU for a particular field. d_{tf} represents the dose to a target t for a specific field f. The field weight optimization was conducted in Matlab (MathWorks, Natick, MA) and iteratively adjusted the field weights (W_f) to match the prescription dose (D_{Rx}) and improve uniformity of field weights across all arcs. The field weight optimization aims to minimize the following dose difference:

$$\Delta D = \left| D_{Rx} - \sum_{f} (d_{tf} \times W_f) \right| \tag{1}$$

The field weights were iteratively adjusted using a Nelder-Mead search algorithm in which a simplex is created, and the vertices are used to minimize multidimensional functions [43]. The created simplex is first reflected and the reflected point is compared to the current best minimum. The vertex with the largest value will then be replaced with a new, smaller vertex, reducing the simplex until the coordinates of a local minimum are found.

The field weight optimization was repeated N times, where N represents the total number of arcs in the treatment plan. The Nelder-Mead algorithm utilized a contraction coefficient of 0.5, in order to determine the strength and rate of minimization and to maintain a practical calculation time. At each optimization iteration, a single field weight is reduced by 50%, creating multiple sets of potential field weight values. The field weights are then used to determine the corresponding MU for each arc and are ranked based on the following criteria: absolute difference in prescription and delivered target dose, standard deviation of the difference in prescription and delivered dose, the number of field weights that have < 10% of the median MU, and the standard deviation of MU per arc. All ranking criteria were given equal weighting and the field weight set with the highest average ranking in all categories was used to determine the final, optimized MU of the treatment plan.

2.4 Limited Inverse Optimization

The newly weighted DCA plan then serves as the starting point for limited inverse optimization. The inverse optimization was performed using Eclipse v.15.6 (Varian Medical Systems, Palo Alto, CA) [44], using photon optimization (PO) algorithm version 15603. The inverse optimization stage differs from conventional VMAT inverse optimization in that the optimizer was limited to multi-resolution (MR) level 4. Restricting the optimizer to MR level 4 allows the MLCs to conform to targets intuitively, similar to a DCA technique, while still allowing small, fine-tuned MLC adjustments [45,46].

2.5 Validation and Plan Comparison

In order to validate the effectiveness and performance of the CAVMAT technique, twenty intracranial SRS cases previously treated with single isocenter VMAT, were selected. All clinical VMAT plans were previously planned by an ABR certified physicist with experience in clinical VMAT SRS planning, utilizing SIMT institutional standards established in previous works [47-49]. All clinical cases were reviewed and approved by the attending physician. All planning was performed in External Beam Planning (Varian

Medical Systems) using Analytical Anisotropic Algorithm. The study aimed to only evaluate cases which utilized a single fraction of 20 Gy to treat targets with a diameter ≤ 2 cm. If a case utilized more than a single fraction, it was replanned to a single fraction of 20 Gy. Forcing all plans to the same prescription and fractionation scheme simplifies reported statistics. The twenty cases were selected such that each treated at minimum 3 targets, with some cases treating a maximum of 7 targets. A minimum of 3 targets was utilized as this allowed for different subgrouping combinations and better tested the CAVMAT technique. Plans were limited to 7 targets due to the time-intensive nature of manually planning for larger numbers of targets. Future work will aim to evaluate large number of targets. The twenty VMAT and CAVMAT plans are summarized below in Table 1.

Table 1: Summary of the 20 cases used for VMAT and CAVMAT comparison

Total Number of Targets	**77**
Number of Targets per Plan (mean ± SD)	3.85 ± 1.18
Total Target Volume	46.29 cc
Total Target Volume per Plan (mean ± SD)	2.31 ± 1.79 cc
Maximum Target Volume	6.02 cc
Minimum Target Volume	0.22 cc

Of the twenty clinical cases, 11 plans featured prescription doses less than 20 Gy or utilized multiple fractions. These plans were also replanned to a single fraction of 20 Gy by an ABR certified physicist utilizing the same single-isocenter VMAT technique that was used for the other clinical VMAT plans.

All clinical cases were replanned with the CAVMAT technique, with the same target geometry as the clinically delivered VMAT plans. Arc geometry, gantry, and couch configurations were not adjusted. The primary difference in the VMAT and CAVMAT plans lies in the adjustment of the collimator angle and in the subgrouping process. While the subgrouping process creates duplicated arcs, unique couch angles are not created. For instance, a VMAT plan might contain 4 arcs with a couch angle for each. The CAVMAT counterpart may feature 8 arcs but will only utilize the same 4 couch angles as the VMAT plan. The collimator angle of the CAVMAT plans was adjusted during the subgrouping process and is the primary geometric difference between the VMAT and CAVMAT plans. In summary, the CAVMAT plans utilize the same treatment geometry as the VMAT counterparts, with the number of arcs at each couch angle equal to the number of subgroups. All plans were normalized such that 100% of the prescription dose covers 99.5% of the combined PTV volume.

The degree of MLC modulation in the VMAT and CAVMAT plans was evaluated and compared using a modulation complexity score (MCS) metric, which was originally designed for IMRT applications [50]. The MCS evaluates the leaf sequence variability (LSV) and aperture area variability (AAV) to assess variation in MLC position, field shape irregularity, and field area. MCS range from 0 to 1.0, with 0 representing an open and modulation-free field and 1.0 representing a highly modulated plan. Eclipse API scripting was used to implement the MCS calculation.

2.5.1 Dose-Volume Analysis

Following planning, the cumulative dose volume histogram (DVH) of both the VMAT and CAVMAT plans were analyzed and compared. The total volume of healthy tissue receiving more than 2.5 Gy ($V_{2.5Gy}$[cc]), V_{6Gy}[cc], V_{12Gy}[cc], V_{16Gy}[cc], maximum dose (Dmax), and total MU were collected and compared. The DVHs were also used to evaluate the limiting coverage of both the VMAT and CAVMAT plans. Limiting coverage was defined as the target with the lowest percentage of volume receiving the prescription dose. Conformity index (CI) was also measured and is defined as the volume enclosed by the prescription isodose surface (V_I) divided by the total target volume (V_t) [51].

$$CI = \frac{V_I}{V_t} \tag{2}$$

A Wilcoxon signed rank test was used to compare the maximum dose, CI, dose-volume statistics, and limiting target coverage of the VMAT and CAVMAT plans. The Wilcoxon test is a non-parametric test and is used to compare matched samples. p values < 0.05 were considered to be statistically significant.

2.5.2 Treatment Time Estimation

The total treatment time for each plan was estimated using the arc control points, dose rate, and gantry speed. Each control point was evaluated, and treatment time was calculated as the summation of the time required to move from one control point to the next [51].

$$\sum_{i=0}^{n} \left(\frac{MU_i}{MaxDoseRate} \text{ or } \frac{Angle_i}{MaxGantrySpeed} \right) \tag{3}$$

The treatment time between two individual control points is determined based on whether dose rate or gantry speed is the limiting factor, as both cannot be maximized simultaneously. The treatment time summation across all control points is calculated based on whether the maximum dose rate or maximum gantry speed restricts the treatment speed more. While MLC velocity can be a limiting factor in some treatment situations, it was not found to contribute to either the VMAT or CAVMAT plans. A Wilcoxon signed rank test was used to compare the maximum dose, CI, dose-volume statistics, and limiting target coverage of the VMAT and CAVMAT plans. The Wilcoxon test is a non-parametric test and is used to compare matched samples. p values < 0.05 were considered to be statistically significant.

2.6 DLG Sensitivity Analysis

A subset of VMAT and CAVMAT plans were selected to be evaluated at different DLG values to simulate an improper or suboptimal selection of DLG value. This analysis aims to quantify the severity of plan degradation with changing DLG and to evaluate CAVMAT's sensitivity to such changes. CAVMAT aims to maintain target coverage and healthy tissue sparing as the DLG value varies, increasing overall technique robustness. Ten of the clinical VMAT and CAVMAT plans, with 46 targets in total, were selected and replanned with DLG values of 0.4mm, 0.8mm, and 1.2mm, creating 60 different plans in total. All plans were first calculated with a DLG value of 0.4 mm in order to establish a baseline for future comparison. A dose grid of 1 mm was used and all plans were recalculated with a constant MU.

The DVH of all 60 plans were evaluated and the V_{6Gy}[cc], V_{12Gy}[cc], V_{16Gy}[cc} of healthy tissue was collected. The minimum, mean, and maximum dose to all 46 targets was also collected. Target volume, equivalent sphere radius, CI, and target distance from radiation isocenter were measured and recorded. The percent change in CI and dose-volume statistics were calculated as the DLG value was changed from 0.4 mm to 0.8 mm, and from 0.4 mm to 1.2 mm, for both the VMAT and CAVMAT plans.

For all 46 targets, target size and distance from isocenter were evaluated to investigate a potential correlation with dosimetric sensitivity for varying DLG values.

2.7 Treatment Delivery and Log File Analysis

Similar to the DLG analysis, a subset of VMAT and CAVMAT plans were delivered to a QA phantom to evaluate how well each plan could be delivered and to quantify the difference in intended and delivered dose. While QA phantoms can be used to evaluate dosimetric deliverability, log file analysis can better attest to MLC motion and positional error, offering a mechanical perspective of treatment delivery error. Ten VMAT and CAVMAT plans, with a constant DLG value of 0.4 mm, were prepared for delivery and uploaded to a Delta^4 (ScandiDos, Madison, WI) QA phantom for delivery. All plans were delivered using the same Varian Trubeam STx (Varian Medical Systems, Palo Alto, CA) that was used for the delivery of the clinical VMAT plans. Following delivery, the delivered (actual) MLC positions of both the VMAT and CAVMAT plans were stored as trajectory log files in the TrueBeam system (Varian Medical Systems, Palo Alto, CA) [52]. The linear accelerator log files were extracted using an in-house script written in Python v.3.7 (Python Software Foundation, Wilmington, DE), utilizing Pylinac, an open-source Python toolkit for linear accelerator–based QA. The script scans the trajectory log files and identifies the delivered MLC and gantry positions for each arc control point [53]. A copy of the original plan was then created and the exported MLC and gantry positions were then overwritten by the recorded log file values. The log file-based plans were calculated with the same MU, AAA, and dose grid size as the original treatment plans.

Similar to the initial DLG analysis, V_{6Gy}[cc], V_{12Gy}[cc], V_{16Gy}[cc], individual target doses were collected. The minimum, mean, and maximum dose to all 41 targets was collected. Target volume, equivalent sphere radius, and distance from radiation isocenter were measured and recorded. CI and limiting coverage were also collected.

The trajectory log files were used to determine the MLC position at each control point of the VMAT and CAVMAT arcs. The MLC positional error at each control point was defined as the absolute difference between planned and delivered MLC positions.

The delivered dose was measured using the Delta[4] phantom for both the VMAT and CAVMAT plans, with Gamma index and dose difference used for comparative analysis. Increasingly strict passing criteria were utilized to assess plan robustness. Gamma analysis was performed using 3%/1mm, 2%/1mm, and 1%/1mm passing criteria.

The distance to agreement (DTA) was held to a constant 1 mm and the dose difference component varied from 3% to 1%. The constant DTA allowed for isolation and evaluation of the dose difference contribution to the gamma analysis.

3. Results

The CAVMAT process resulted in conformal MLC trajectories inherent to DCA to maximize collimation between targets and to eliminate irregular MLC openings. One of the 20 cases was selected and is displayed below in detail to demonstrate the differences in the collimation and dose-volume statistics of a typical CAVMAT plan, compared to its VMAT counterpart.

3.1 Sample Case

The conformal MLC trajectories and target subgrouping for a sample arc is displayed below in Figure 3 and is compared to its VMAT counterpart.

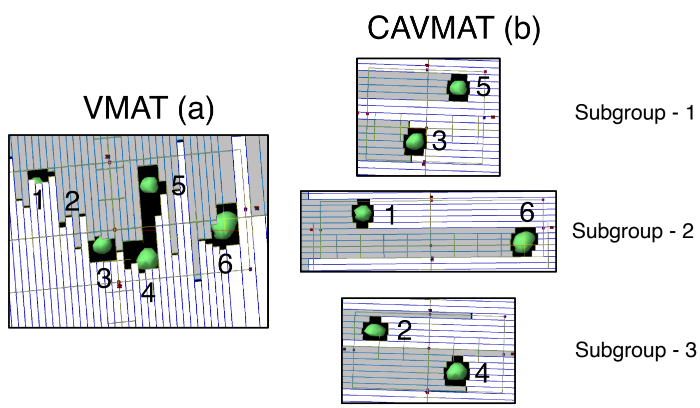

Figure 3: Irregular MLC trajectories and openings of VMAT (a) and conformal subgrouping of CAVMAT (b)

In many treatment scenarios and geometries, VMAT may utilize nonconformal MLC trajectories when struggling to shield between targets. By placing the targets of a treatment arc into subgroups, CAVMAT can improve MLC blocking between targets by allowing the MLCs to conform closely. The use of target subgroups allows for conformal MLC trajectories that do not become highly modulated following inverse optimization.

As seen in Figure 3a above, the MLC trajectories of the VMAT plan creates irregular MLC openings both on and around the six targets. A substantial MLC opening is present between targets 4 and 5, targets 1, 3, 4, and 6 are partially blocked, and target 2 is completely blocked by the MLCs. In comparison, CAVMAT utilizes 3 subgroups, of 2 targets each, with effective collimation.

For the same sample case, the isodose distribution and corresponding DVH of the VMAT, pre-, and post-inverse optimized CAVMAT treatment plan is displayed below in Figure 4. The irregular and nonconformal MLC trajectories of VMAT may increase the likelihood of irregular MLC openings, which may lead to dose bridging and an increased healthy tissue dose. The effect of the irregular MLC motions can be seen in the dose distribution in Figure 4a. Compared to VMAT, CAVMAT was able to produce isodose distributions that are both intuitive and concentric, improving healthy tissue sparing.

In this example, the VMAT plan yields an irregular-shaped and nonintuitive dose distribution, with dose bridging of 6 and 10 Gy between targets such that tissue is unnecessarily irradiated, and some targets receive over 110% of the prescription dose of 20 Gy, as seen in Figure 4a.

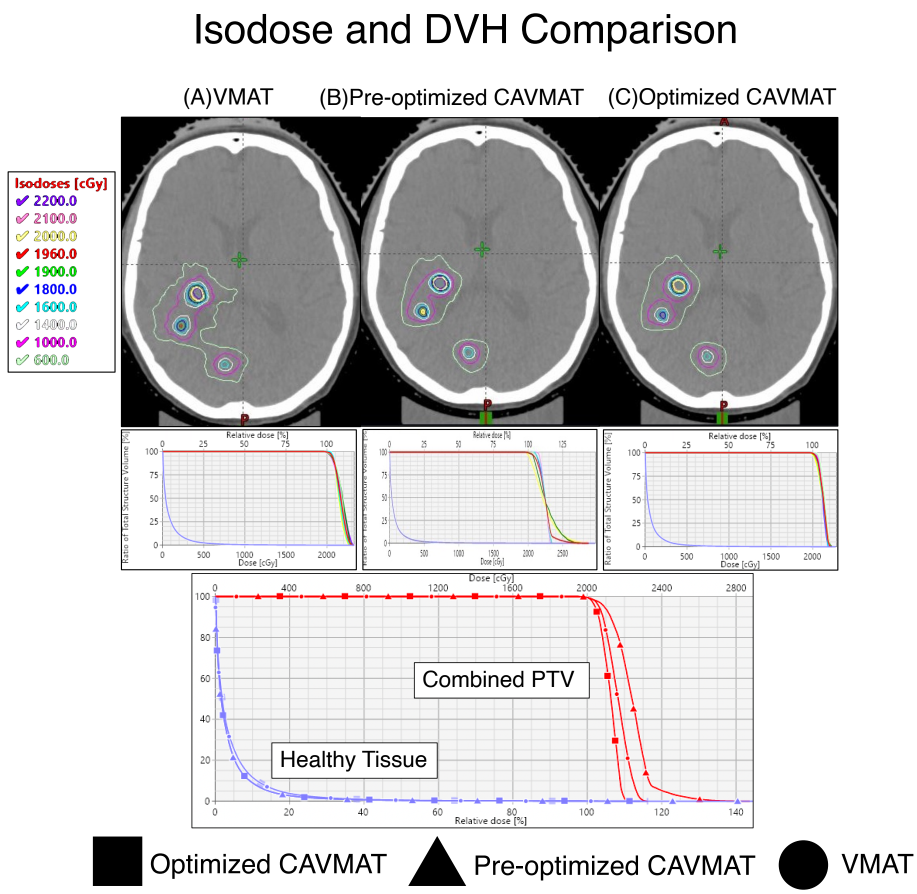

Figure 4: VMAT (A) provides uniform target dose at the cost of dose bridging and an irregular dose distribution. Pre-optimized CAVMAT (B) reduces dose bridging but struggles to maintain dose and conformity. Inverse Optimized CAVMAT (C) combines the benefits of both.

The pre-optimized CAVMAT plan (Figure 4b) is capable of eliminating or mitigating the dose bridging of 6 Gy and further constrains the 10 Gy dose bridging between the 2 targets in close proximity. It also produces a smoother dose distribution than the VMAT plan, eliminating many of the rough edges and increasing healthy tissue sparing. For this sample case, the pre-optimized CAVMAT plan reduced the $V_{2.5Gy}$[cc] of heathy tissue by 26.08% (82.18cc), V_{6Gy}[cc] by 27.71% (17.49 cc), V_{12Gy}[cc] by 28.21% (3.77cc), and V_{16Gy}[cc] by 11.33% (0.69 cc). While the pre-optimized CAVMAT plan substantially spares tissue, large heterogeneities can be seen in DVH B of Figure 4b. Large heterogeneities prior to inverse optimization were found to be common, as the field weight optimization considers dose and MU to create a starting point for inverse optimization, but does not explicitly consider conformity and other parameters.

The inverse optimized CAVMAT plan (Figure 4c) produces a more concentric, smooth, and less heterogenous dose distribution than both the pre-optimized CAVMAT and VMAT plans.

3.2 Cumulative Results

Considering all 20 cases, the pre-optimized CAVMAT plans were able to substantially spare healthy tissue, effectively reducing $V_{2.5Gy}$ [cc] of heathy tissue by 30.39 ± 20.04% (79.52 cc), V_{6Gy}[cc] by 23.06 ± 22.41% (38.86 cc), V_{12Gy}[cc] by 17.34 ± 20.23% (11 cc) and V_{16Gy}[cc] by 7.52 ± 19.78 % (6.69 cc). While the pre-optimized CAVMAT plan slightly increased healthy tissue sparing, it accomplishes this at the cost of degraded conformity. The 20 pre-optimized CAVMAT plans produced an increased average conformity index of 1.63 ± 0.32 compared to 1.40 ± 0.19 for the VMAT counterparts. Figure 4b above demonstrates the degraded conformity of the pre-optimized CAVMAT plans, a trend that was observed across all 20 plans. The total MU of the pre-optimized CAVMAT plans increased by 29.40 ± 26.40%. The degraded conformity of the pre-optimized CAVMAT plans necessitates the inverse optimization stage.

Figure 5 illustrates the healthy tissue sparing of the optimized CAVMAT plans.

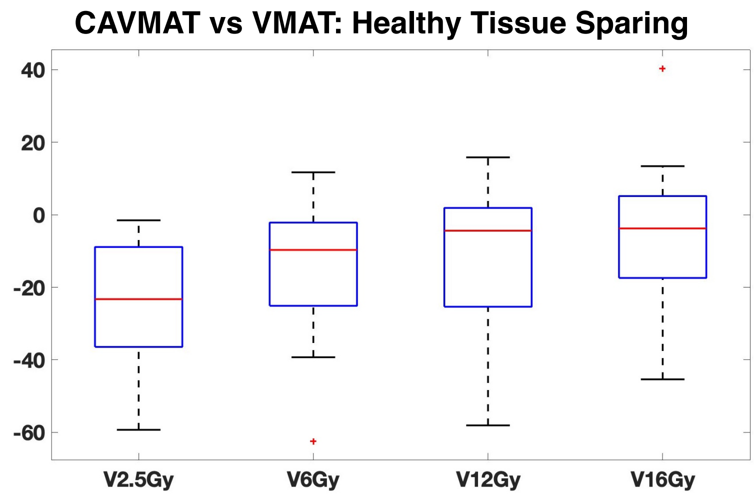

Figure 5: Average Percent change between VMAT and CAVMAT

Compared to VMAT, the optimized CAVMAT plans were able to reduce $V_{2.5Gy}$[cc] of total tissue by 25.25 ± 19.23% (66.35 ± 58.93 cc) (p=8.85 x 10^{-5}), V_{6Gy}[cc] by 13.68 ± 18.97% (6.33 ± 5.07 cc) (p=0.027), V_{12Gy}[cc] by 11.40 ± 19.44% (1.32 ± 1.12 cc) (p=0.048), and V_{16Gy}[cc] by 6.38 ± 19.11% (0.63 ± 0.38 cc) (p=0.247). As displayed below in Figure 6, the optimized CAVMAT plans produced an average conformity index of 1.34 ± 0.15 compared to 1.40 ± 0.19 for VMAT.

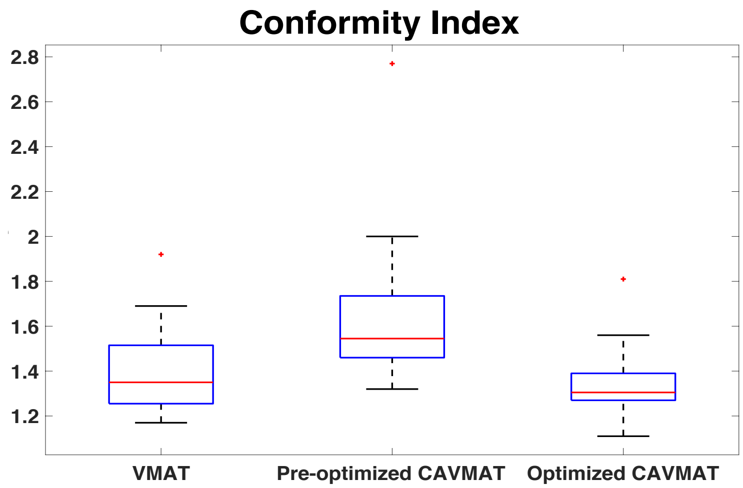

Figure 6: Pre-optimized CAVMAT results in an increased average conformity of 1.63±0.32, while optimized CAVMAT produces more conformal plans, improving conformity from 1.40±0.19 for VMAT to 1.34±0.15

A comparison of the limiting target coverages of the optimized CAVMAT and VMAT plans yielded a p value of 0.49, demonstrating that a significant difference was not found and that CAVMAT is capable of maintaining comparable coverage. The optimized CAVMAT plans utilized roughly 5% less MU than the pre-optimized plans, as inverse optimization further modulates the MU applied to each control point to improve plan quality. The average total MU of the optimized CAVMAT plans was increased 24.35 ± 24.66% (1507.70 ± 1182.23) compared to the VMAT plans. The dose-volume, conformity index, and MU data are compiled in Table 2 to further illustrate the differences in VMAT, pre-, and post-optimized CAVMAT plans.

Table 2: Summarized metrics for VMAT, pre, and post-optimized CAVMAT comparison

	VMAT	Pre-optimized CAVMAT	Post-Optimized CAVMAT
$V_{2.5\ Gy\ [cc]}$	294.94 ± 170.42 cc	213.41 ± 142.52 cc	226.59 ± 143.83 cc
$V_{6\ Gy\ [cc]}$	46.19 ± 24.92 cc	38.86 ± 27.94 cc	41.99 ± 26.15 cc
$V_{12\ Gy\ [cc]}$	12.43 ± 6.09 cc	11.00 ± 6.92 cc	11.62 ± 6.90 cc
$V_{16\ Gy\ [cc]}$	6.81 ± 3.79 cc	6.69 ± 4.31 cc	6.63 ± 4.15 cc
CI	1.40 ± 0.19	1.63 ± 0.32	1.34 ± 0.15
MU	6117.50 ± 1165.61	7696.55 ± 1545.41	7289.40 ± 1474.81
Tx Time	7.82 ± 3.15 min		9.70 ± 3.33 min

The average estimated treatment delivery time of the 20 CAVMAT plans was 9.47 ± 3.18 min compared to 7.82 ± 3.15 for the VMAT plans. The increased treatment time is within reason, as the CAVMAT plans have an average of 7.55 ± 1.85 arcs per plan compared to 3.75 ± 0.64 arcs for the VMAT plans. While the CAVMAT plans have roughly twice as many arcs, the average estimated treatment time was not doubled because unique arcs, couch, and gantry angles were not created; the additional arcs are duplicate arcs of the base VMAT plan. Both the VMAT and CAVMAT plans have identical plan geometry, with the CAVMAT plans rotating the gantry clockwise and then counterclockwise at each couch angle to deliver the subgroup arcs. It was observed that the VMAT plan delivery was almost always limited by dose rate and CAVMAT delivery was limited by gantry rotation speed. The treatment time was not limited by the MLC speed.

3.2.1 Effect of varying MLC and Jaw sizes

Prior to the full plan comparison, the ideal MLC and jaw margins were determined. The 20 CAVMAT plans were replanned with a uniform 2 mm MLC and jaw setting to establish a baseline and was found to offer no tissue sparing benefit. Table 3 illustrates the effect of MLC and jaw margin setting on the pre-optimized CAVMAT plans.

Table 3: MLC and jaw margins for pre-optimized CAVMAT

Pre-Optimized CAVMAT - Plan Comparison						
% Change From VMAT						
Jaw Margin	**MLC Margin**	**V6**	**V12**	**V16**	**CI (absolute values)**	**MU**
2mm	**2mm**	12.93 ± 37.65%	21.02 ± 32.19%	36.11 ± 30.10%	2.33 ± 0.77	17.42 ± 25.51%
1mm	**1mm**	-24.02 ± 20.41%	-16.91 ± 21.46%	-6.79 ± 21.27%	1.53 ± 0.20	28.53 ± 27.95%
3mm	**1mm**	-23.06 ± 22.41%	-17.34 ± 20.23%	-7.52 ± 19.78%	1.63 ± 0.32	29.40 ± 26.40%
	VMAT				1.40 ± 0.19	

Prior to inverse optimization, the pre-optimized CAVMAT plans, featuring a uniform 1 mm MLC and jaw setting offered substantial tissue sparing. Following inverse optimization, the 2 mm MLC and jaw fit demonstrated substantially improved conformity, while the 1 mm fit demonstrated only a slight improvement. Table 4 illustrates the effect of MLC and jaw margin setting on the post-optimized CAVMAT plans.

Table 4: MLC and jaw margins for post-optimized CAVMAT

Post-Optimized CAVMAT - Plan Comparison						
% Change From VMAT						
Jaw Margin	MLC Margins	V6	V12	V16	CI (absolute values)	MU
2mm	2mm	11.34 ± 23.83%	17.40 ± 21.43%	25.56 ± 19.78%	1.73 ± 0.64	18.37 ± 27.37%
1mm	1mm	-22.90 ± 21.50%	-16.64 ± 21.40%	-8.24 ± 19.76%	1.48 ± 0.28	28.98 ± 26.93%
3mm	1mm	-13.68 ± 18.97%	-11.40 ± 19.44%	-6.38 ± 19.11%	1.34 ± 0.15	24.35 ± 24.66%
	VMAT				1.40 ± 0.19	

The 1 mm MLC and jaw fit was found to be problematic during the inverse optimization stage, as MLC leaf pairs were often prevented from opening to the full field size. This was particularly apparent in target subgroups featuring only 1 or 2 targets, as smaller field sizes were used, and the MLCs struggled to conform to targets properly. The use of small fields often created static leaf pairs. This often resulted in undercoverage of 1 or more targets and was visually apparent in the DVH.

A jaw setting of 3 mm and 1 mm MLC margins was found to preserve the majority of the tissue sparing benefits of the 1mm uniform fit, while improving conformity substantially. The larger jaw setting creates a larger field size and allows MLC leaf pairs to conform correctly when smaller fields are utilized. The 3 mm jaw setting and 1 mm MLC margins allows CAVMAT to produce a conformity that is slightly improved compared to VMAT and to spare healthy tissue substantially.

3.3 Robustness to Uncertainties in Dosimetric Leaf Gap

Of the 10 cases and 46 targets tested at DLG values of 0.4 mm, 0.8 mm, and 1.2 mm, a sample case was selected to demonstrate the impact of a varying DLG. Figure 7 below illustrates the DVH of a single VMAT and CAVMAT plan featuring 4 targets. The DVHs display the combined PTV structures of both plans at all 3 DLG values.

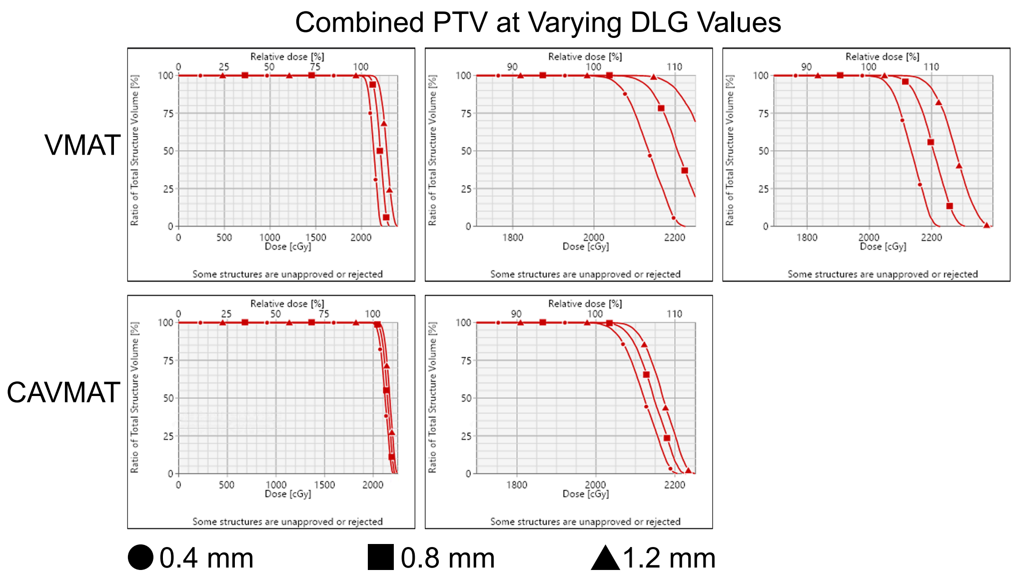

Figure 7: CAVMAT demonstrates an increased resistance to variation in DLG value. A third closer view of the VMAT plan is displayed

For this example case, the VMAT plan was roughly twice as sensitive to changes in DLG value than the CAVMAT plan. For an increasing DLG, the VMAT plan demonstrated a sensitivity to changes in V_{6Gy}[cc], V_{12Gy}[cc], V_{16Gy}[cc] of 33.2 $\frac{\%}{mm}$, 34.72 $\frac{\%}{mm}$, and 43.96 $\frac{\%}{mm}$, compared to 21.95 $\frac{\%}{mm}$, 22.33 $\frac{\%}{mm}$, and 26.11 $\frac{\%}{mm}$ for the CAVMAT plan, respectively. Similarly, the maximum, mean, and minimum dose of each target in the VMAT plan in this example case was found to be more sensitive than the CAVMAT plan to changes in DLG. The VMAT plan demonstrated an average sensitivity to changes in maximum, mean, and minimum dose of 8.33 $\frac{\%}{mm}$, 9.15 $\frac{\%}{mm}$, and 8.63 $\frac{\%}{mm}$, respectively, compared to 2.52 $\frac{\%}{mm}$, 4.23 $\frac{\%}{mm}$, and 3.0 $\frac{\%}{mm}$ for the CAVMAT plan, respectively.

The trends observed in the sample case were present across all 10 plans. The 10 VMAT plans demonstrated an average sensitivity in V_{6Gy}[cc], V_{12Gy}[cc], V_{16Gy}[cc] of 35.83 ± 9.48 $\frac{\%}{mm}$, 34.12 ± 6.61 $\frac{\%}{mm}$, and 39.22 ± 8.41 $\frac{\%}{mm}$, respectively, compared to 23.18 ± 4.53 $\frac{\%}{mm}$, 22.45 ± 4.28 $\frac{\%}{mm}$, and 24.88 ± 4.91 $\frac{\%}{mm}$ for CAVMAT, respectively.

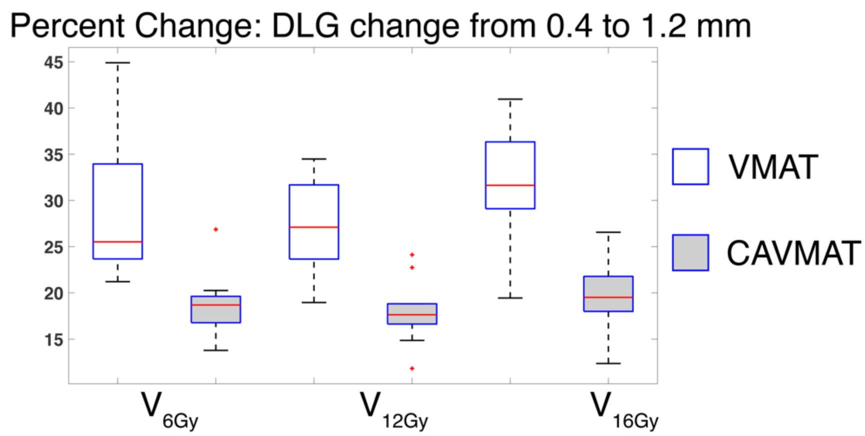

Figure 8: Reduced sensitivity of CAVMAT to changes in V_{6Gy}[cc], V_{12Gy}[cc], and V_{16Gy}[cc] for a DLG change of 0.4 mm to 1.2mm

The average VMAT sensitivity to changes in maximum, mean, and minimum dose following a change in DLG, was found to be 9.08 ± 3.45 $\frac{\%}{mm}$, 9.22 ± 3.23 $\frac{\%}{mm}$, and 9.5 ± 3.25 $\frac{\%}{mm}$, respectively, compared to an average of 3.2 ± 1.63 $\frac{\%}{mm}$, 3.50 ± 1.35 $\frac{\%}{mm}$, and 4.72 ± 1.63 $\frac{\%}{mm}$ for CAVMAT, respectively.

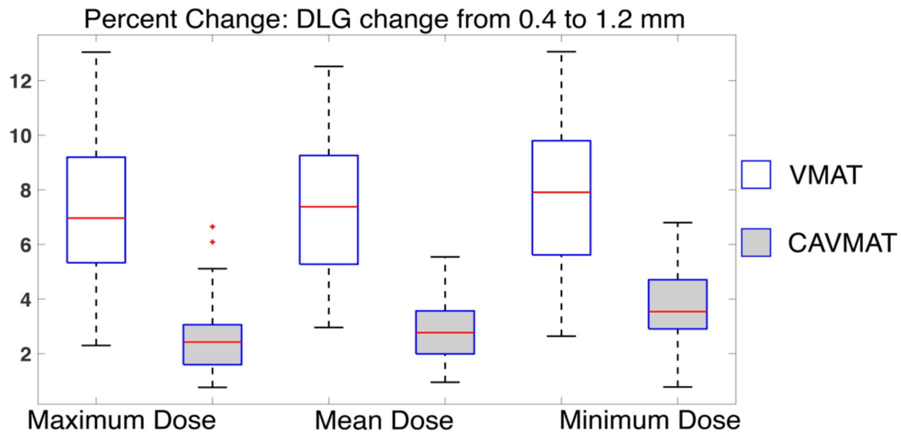

Figure 9: Reduced sensitivity of CAVMAT to changes in target dose, for a DLG change of 0.4 mm to 1.2 mm

A paired sample T-test demonstrated that a statistically significant correlation between target size, distance from isocenter, and dosimetric sensitivity to variation in DLG was not found.

The 10 VMAT and CAVMAT plans were evaluated using the MCS algorithm and a constant DLG value of 0.4 mm. The VMAT plans demonstrated an average MCS score of 0.036 ± 0.019 with an average equivalent field size of 1.51 ± 0.42 cm^2 for each arc. In comparison, the CAVMAT plans were found to be less modulated, with an average MCS score of 0.052 ± 0.031, but with a smaller average equivalent field size of 1.11 ± 0.43 cm^2 for each arc.

3.4 Treatment Delivery Robustness

10 VMAT and CAVMAT plans were selected and delivered to the Delta4 phantom. For the VMAT plans, the log file analysis indicated the average V_{6Gy}[cc] increased by 0.93

± 1.43%, V_{12Gy}[cc] increased by 0.90 ± 1.38%, and V_{16Gy}[cc] increased by 1.23 ± 1.54%. In comparison, the average V_{6Gy}[cc] for CAVMAT decreased by 0.035 ± 0.14%, while the V_{12Gy}[cc] and V_{16Gy}[cc] increased by 0.14 ± 0.18% and 0.28 ± 0.24%, respectively.

The post-delivery VMAT and CAVMAT plans both demonstrated small changes in maximum, mean, and minimum target dose. For the VMAT plans, the average maximum, mean, and minimum target dose increased by 0.53 ± 0.46%, 0.52 ± 0.46%, and 0.53 ± 0.56%, compared to an increase of 0.16 ± 0.18%, 0.11 ± 0.08%, and 0.07 ± 0.11%, for CAVMAT plans, respectively. The VMAT plans were more sensitive to change in conformity index, with an increase of 3.74 ± 3.42%, from 1.48 ± 0.21 to 1.54 ± 0.24. In comparison, the conformity index for the CAVMAT plans increased by 0.79 ± 0.65%, from 1.38 ± 0.19 to 1.39 ± 0.19.

The average target coverage of the VMAT and CAVMAT plans was comparable, with VMAT coverage changing by 0.15 ± 0.24% (99.50% to 99.65% coverage) following delivery, compared to a 0.01 ± 0.28% (99.65% to 99.67% coverage) change for the CAVMAT plans.

Similarly, the 10 VMAT and CAVMAT plans were comparable in terms of MLC and gantry positioning error; substantial variation was not found in either sets of plans. The absolute average MLC positional error of the VMAT plans was 0.017 ± 0.012 mm, compared to 0.023 ± 0.019 mm for the CAVMAT plans.

For the same 10 delivered plans, gamma analysis was performed with an increasingly strict 3%/1mm, 2%/1mm, and 1%/1mm passing criteria. For the 3%/1mm test, the VMAT plans demonstrated an average passing rate of 99.61 ± 0.43%% compared to 99.98 ± 0.06% for CAVMAT. As seen below in Figure 10, the VMAT plans' passing rate changed substantially for an increasingly strict passing criterion.

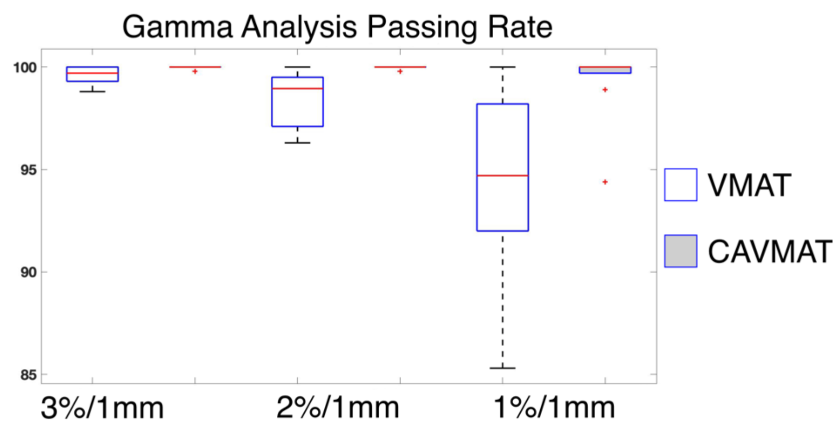

Figure 10: CAVMAT's reduced sensitivity to changes in gamma analysis passing rate

For a 2%/1mm test criteria, the average VMAT passing rate was 98.54 ± 1.29% compared to 99.98 ± 0.06% for CAVMAT. Furthermore, for a stricter criterion of 1%/1mm, the average VMAT gamma analysis passing rate was 94.53 ± 4.42% compared to 99.28 ± 1.74% for CAVMAT.

For the plans delivered to the Delta[4] phantom, the dose difference component of the gamma analysis was isolated and is displayed below in Figure 11 for both the VMAT and CAVMAT plans.

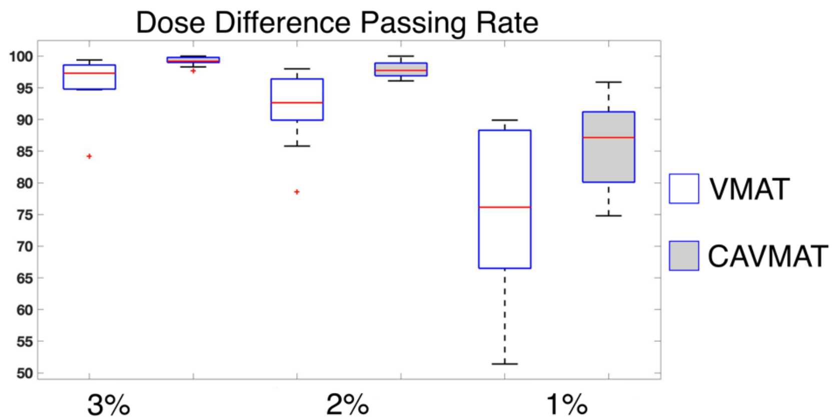

Figure 11: Dose difference passing rate of CAVMAT versus VMAT for the plans delivered to the Delta[4]

For a 3% dose difference criterion, the average passing rate of the VMAT plans was 96.03 ± 4.44% compared to 99.17 ± 0.74% for CAVMAT. By increasing dose difference criteria to 2%, the VMAT average passing criteria decreased to 91.74 ± 5.89%, compared to 97.91 ± 1.36% for CAVMAT. For the strictest criteria of 1% dose agreement, the average VMAT passing rate was further reduced to 74.78 ± 13.00%, compared to 86.16 ± 6.38% for CAVMAT.

4. Discussion

While SRS techniques are capable of effectively treating and controlling malignant disease, radiation treatments may induce neurological complications [53]. Radionecrosis is a common side effect in a substantial percentage of SRS patients and may be associated with speech, motor, and other neurological deficits [54]. In SRS applications, the V_{6Gy}[cc], V_{12Gy}[cc], and V_{16Gy}[cc] dose-volume thresholds are often used to assess the relative risk of radionecrosis and neurocognitive decline [53,55,56]. For this study, the CAVMAT treatment planning technique reduced the average $V_{2.5Gy}$[cc], V_{6Gy}[cc], V_{12Gy}[cc], and V_{16Gy}[cc] of the total volume by 25.25 ± 19.23%,13.68 ± 18.97%, 11.40 ± 19.44, and 6.38 ± 19.11% respectively, potentially reducing the risk of radionecrosis and neurological complications.

Sufficient modeling of dose-volume parameters in the treatment planning system is crucial for the accurate determination of post-treatment complications. Lower dose values, like V_{6Gy}[cc] and V_{12Gy}[cc], lie in the penumbra region of the beam, where tissue exhibits a greater dose uncertainty [57]. The clinical importance of these dose-volume parameters highlights the necessity for treatment planning techniques that are less sensitive to these uncertainties.

Proper treatment planning system configuration is crucial to the delivery of accurate and effective treatment plans [58]. The use of small radiation fields, as found in VMAT, may further complicate the configuration process and the dosimetric accuracy of a treatment [32]. Accurately modeling the dosimetric leaf gap (DLG) poses a challenge as it can drastically affect treatment plan quality [26].

Numerous studies have investigated the commissioning process of determining the DLG value using set field sizes and the sweeping gap technique. In most cases the DLG value measured at commissioning does not provide a sufficiently close match between measured and calculated dose, necessitating a further correction of the DLG [36,59,60]. In some instances, failing to correct the calculated DLG value may lead to a difference in measured and calculated dose on the order of 5% [59]. While differing DLG values may be required for different types of radiation treatment, some institutional studies have even reported difficulty in determining a single DLG value that is sufficient for all of the institutions' radiosurgery cases [37,38]. The potential for substantial dose discrepancies and the fact that a single DLG value cannot sufficiently model all treatment plans of a similar type, necessitates a treatment technique that is resistant to DLG variation.

If systematic error exists in the choice of DLG, or for cases where the optimal DLG varies between plans or between targets within a single plan, the dosimetric impact may be reduced by using the CAVMAT treatment planning technique as our results indicate that CAVMAT is more robust and less sensitive to DLG errors compared to a conventional VMAT technique. For a DLG change of 0.4 to 1.2 mm, the average V_{6Gy}[cc], V_{12Gy}[cc], and V_{16Gy}[cc] of the VMAT plans increased by 35.83 ± 9.48 $\frac{\%}{mm}$, 34.12 ± 6.61 $\frac{\%}{mm}$, and 39.22 ± 8.41 $\frac{\%}{mm}$ respectively. In comparison, the average V_{6Gy}[cc], V_{12Gy}[cc], and V_{16Gy}[cc] of the CAVMAT plans increased by 23.18 ± 4.53 $\frac{\%}{mm}$, 22.45 ± 4.28 $\frac{\%}{mm}$, and 24.88 ± 4.91 $\frac{\%}{mm}$ respectively. The max dose applied to each target increased by 9.08 ± 3.45 $\frac{\%}{mm}$ for VMAT and 3.2 ± 1.63 $\frac{\%}{mm}$ for CAVMAT. Thus, for these cases when the value of the DLG was modified CAVMAT was more effective in maintaining the planned doses to healthy tissues as well as the coverage and dose applied to each target.

The highly modulated MLC trajectories inherent to complex, conventional treatment plans, have been shown to reduce the dosimetric accuracy and effectiveness of a given plan [24,25]. On average the CAVMAT plans produce a larger MCS score, correlating with a reduced plan complexity, compared to VMAT plans. The reduced plan complexity is likely a trait inherent to CAVMAT, as target subgrouping promotes intuitive and conformal MLC trajectories. In addition, the inverse optimization stage of the CAVMAT process is restricted to MR (multi-resolution) level 4, which further prevents highly modulated MLC trajectories.

While errors may arise from improper beam configuration, uncertainly may also be inherently present in the treatment delivery process. In some scenarios, the physical motion of the MLCs may differ from the intended motion defined in the treatment plan. Variation in MLC motion can be due to gravitational effects as well as the speed of leaf pair extension and contraction. Previous studies have used a similar log file analysis methodology to investigate the dosimetric impact of MLC position and gantry rotation errors, however, the primary focus was on head and neck or prostate cancer [61,62]. While our study analyzes MLC positional error in a similar manner, the primary focus is multiple brain metastases, treated with a single isocenter. In our study, the MLC positional error for both the VMAT and CAVMAT plans was found to be small and comparable, demonstrating that the linear accelerator is capable of delivering CAVMAT and VMAT plans effectively. While CAVMAT was found to be more robust than VMAT and better capable of maintaining the dose and coverage to each target than VMAT, the percentage differences were slight and unlikely to have clinical significance. While the differences in target doses and dose-volume statistics were not large, the gamma analysis portion of the study demonstrated that the CAVMAT technique provided a greater overall agreement between planned and delivered dose than VMAT. The CAVMAT technique offered a superior gamma analysis passing rate for each gamma analysis criteria, particularly at the 1%/1mm test. The dose difference passing rate followed a similar trend, demonstrating that CAVMAT is capable of a greater dose agreement than VMAT, even with increasingly strict passing criteria. The difference in agreement for the measurement may be related to the sensitivity to beam configuration for the two types of plans, given the minimal effect observed from the log file analysis.

From a plan quality perspective, the inherent benefit of CAVMAT is not necessarily a result of utilizing more arcs, as a VMAT plan with the same number of arcs would still suffer from the geometric challenge of blocking healthy tissue between targets. CAVMAT overcomes these limitations by utilizing target sub-grouping and optimal field weighting, to create an intuitive starting point for inverse optimization.

While other studies and institutions have utilized hybrid treatment planning techniques that lie between conformal arc treatments and conventional VMAT, CAVMAT is unique in the use of target subgrouping and the Varian VMAT optimization [63,64]. CAVMAT also differs from previous hybrid techniques in that it offers substantial healthy tissue sparing. Several commercial treatment techniques have been developed to improve upon multi-target radiosurgery. Brainlab Elements is an automated software solution which aims to treat multiple targets with pre-configured sets of dynamic conformal arcs. At each couch angle, two separate arcs are created, potentially producing treatment time on par with CAVMAT [65]. While CAVMAT and Elements share a target subgrouping component, both techniques employ a different methodology and criteria to subgroup targets [54]. Elements is conceptually similar to CAVMAT prior to inverse optimization, while the limited inverse optimization of CAVMAT adds flexibility in MLC modulation to adjust for complex geometries and further improve dose conformity. Varian Medical Systems has implemented several different treatment techniques to improve the quality of radiosurgery, such as RapidPlan and HyperArc. RapidPlan allows for automated creation of VMAT plans, while HyperArc uses a single isocenter VMAT treatment and an automated planning process to optimize couch, collimator, and beam arrangement settings [66-68]. Future work aims to compare CAMAT to Elements, RapidPlan, and HyperArc.

The CAVMAT treatment planning process is robust in that any dose can be used, with the only required adjustment occurring in the field weight optimization and inverse optimization constraints.

4.1 Limitations

The CAVMAT technique is limited by the subgrouping process and the manual determination of optimal collimator angles to prevent dose bridging. The subgrouping process may become particularly time consuming and intensive in treatment scenarios including a large number of targets, targets of differing depths, and or challenging target geometry. In some instances, target superposition may become unavoidable without an excessive number of subgroups per arc. The nature of the manual selection of subgroups may introduce plan variability, as different planners may utilize different subgroups, potentially affecting the total number of arcs, treatment time, and overall plan quality. Manual target subgrouping leads to an estimated treatment planning time of toughly 1 – 1.5 hrs for an experienced planner, with variability for cases with a large number of targets. Of the 20 VMAT and CAVMAT plans that were used for the initial plan comparison portion of the study, each plan contained between 3-7 targets and only 4 plans required an arc with 3 subgroups to sufficiently treat all targets. All other plans were capable of meeting treatment goals with 2 subgroups for each arc. A direct correlation between total target number and plan quality was not found, as plan quality may depend on target position and geometry. In complex cases treating a large number of targets, many subgroups may be required, potentially reducing plan practicality.

In terms of the DLG analysis and the 10 delivered VMAT and CAVMAT plans, there are other beam configuration parameters and general treatment errors that were not evaluated. Future work may investigate planning and delivery sensitivity to changing focal spot sizes and the commissioning of MLC transmission factors. Future work may utilize different detectors or phantoms, as the Delta[4] is constructed of a diode array and is limited in spatial resolution.

4.2 Potential Applications

CAVMAT has the potential to be applied by institutions currently using VMAT and the same treatment planning system. The time-consuming nature of the manual CAVMAT process may restrict routine use in a clinical setting, however, a feasible clinical workflow could be facilitated in future work by applying the technique through scripting in the treatment planning system or through refinement of the Matlab field weight optimization script such that it can easily be distributed for use at other institutions. Partial or complete automation of the subgrouping process could substantially reduce the treatment planning time and further improve plan quality by ensuring optimal selection of subgroups and collimator angles. Previous work has demonstrated the feasibility of using scripting techniques to determine the optimal collimator angle for cases involving multiple targets [66]. Automation is possible through Eclipse Scripting API and is currently under development.

5. Conclusion

By pairing the conformal MLC motions of DCA plans with flexible MLC modulation of limited inverse optimization, CAVMAT can produce clinically viable plans with similar quality (low dose sparing & conformity) to standard radiosurgery techniques but with decreased plan complexity. Prior to inverse optimization, CAVMAT further improves healthy tissue sparing but suffers from a degraded target conformity. The plan comparison between VMAT and CAVMAT demonstrates that CAVMAT may be a promising treatment planning strategy for multi-target radiosurgery applications. The clinical feasibility and potential impact of CAVMAT may be bolstered by future investigations into automation. Additional comparisons with other radiosurgery techniques may further highlight the benefit and utility of CAVMAT.

SRS treatment techniques often employ small radiation fields, which may complicate and reduce dosimetric and treatment accuracy. Additionally, the inherent uncertainty of small radiation fields may exacerbate existing treatment and dosimetric uncertainties. Dosimetric uncertainty may arise from the incorrect measurement or suboptimal choice of the dosimetric leaf gap, resulting in changes in the dose to healthy tissue and targets. In the event that a suboptimal DLG is selected, CAVMAT will better maintain the original plan quality and target prescription dose to a greater degree than conventional VMAT techniques.

Uncertainty in MLC motion may arise during treatment delivery. The CAVMAT technique is less sensitive to discrepancies in the intended and delivered MLC motions. Compared to conventional VMAT techniques, CAVMAT better maintains the prescription dose to each target and resists increases in the total volume of tissue receiving low doses following treatment delivery. While the effect of the MLC positional error was minimal, gamma analysis demonstrates that the CAVMAT technique offers a reduced sensitivity to configuration and treatment delivery errors, all while maintaining a superior agreement between calculated and measured dose.

The superior tissue sparing and robust nature of CAVMAT makes the technique a viable and effective approach for single isocenter radiosurgery of multiple brain metastases.

References

[1] Taillibert, S., & Le Rhun. (2015). Epidemiology of brain metastases. Cancer/Radiotherapie, 19(1), 3–9. https://doi.org/10.1016/j.canrad.2014.11.001

[2] Soiza, R. L., Donaldson, A. I. C., & Myint, P. K. (2018). Vaccine against arteriosclerosis: an update. Therapeutic Advances in Vaccines, 9(6), 259 261.https://doi.org/10.1177/https

[3] Patchell RA, Tibbs PA, Regine WF, et al. Postoperative Radiotherapy in the Treatment of Single Metastases to the Brain: A Randomized Trial. JAMA. 1998;280(17):1485–1489. doi:10.1001/jama.280.17.1485

[4] Suteu P, Fekete Z, Todor N, Nagy V. Survival and quality of life after whole brain radiotherapy with 3D conformal boost in the treatment of brain metastases. Med Pharm Rep. 2019;92(1):43–51. doi:10.15386/cjmed-1040

[5] Andrews DW, Scott CB, Sperduto PW, et al. Whole brain radiation therapy with or without stereotactic radiosurgery boost for patients with one to three brain metastases: Phase III results of the RTOG 9508 randomised trial. Lancet. 2004. doi:10.1016/S0140-6736(04)16250-8

[6] Chang EL, Wefel JS, Hess KR, et al. Neurocognition in patients with brain metastases treated with radiosurgery or radiosurgery plus whole-brain irradiation: a randomised controlled trial. Lancet Oncol. 2009. doi:10.1016/S1470-2045(09)70263-3

[7] Brown, P. D., Jaeckle, K., Ballman, K. V., Farace, E., Cerhan, J. H., Keith Anderson, S., … Asher, A. L. (2016). Effect of radiosurgery alone vs radiosurgery with whole brain radiation therapy on cognitive function in patients with 1 to 3 brain metastases a randomized clinical trial. JAMA - Journal of the American Medical Association, 316(4), 401–409. https://doi.org/10.1001/jama.2016.9839

[8] Yamamoto M, Serizawa T, Shuto T, et al. Stereotactic radiosurgery for patients with multiple brain metastases (JLGK0901): A multi-institutional prospective observational study. Lancet Oncol. 2014. doi:10.1016/S1470-2045(14)70061-0

[9] Gevaert T, Steenbeke F, Pellegri L, Engels B, Christian N, Hoornaert MT, Verellen D, Mitine C, De Ridder M. Evaluation of a dedicated brain metastases treatment planning optimization for radiosurgery: a new treatment paradigm?. Radiation Oncology. 2016 Dec;11(1):13.

[10] Huang, Y., Chin, K., Robbins, J. R., Kim, J., Li, H., Amro, H., … Ryu, S. (2014). Radiosurgery of multiple brain metastases with single-isocenter dynamic conformal arcs (SIDCA). Radiotherapy and Oncology, Vol. 112, pp. 128–132. https://doi.org/10.1016/j.radonc.2014.05.009

[11] Clark GM, Popple RA, Young PE, Fiveash JB. Feasibility of Single-Isocenter Volumetric Modulated Arc Radiosurgery for Treatment of Multiple Brain Metastases. Int J Radiat Oncol Biol Phys. 2010;76(1):296-302. doi:10.1016/j.ijrobp.2009.05.029

[12] G.M. Clark, R.A. Popple, B.M. Prendergast, S.A. Spencer, E.M. Thomas, J.G. Stewart, et al. Plan quality and treatment planning technique for single isocenter cranial radiosurgery with volumetric modulated arc therapy Pract Radiat Oncol, 2 (2012), pp. 306-313

[13] C. Audet, B.A. Poffenbarger, P. Chang, P.S. Jackson, R.E. Lundahl, S.I. Ryu, et al. Evaluation of volumetric modulated arc therapy for cranial radiosurgery using multiple noncoplanar arcs Med Phys, 38 (2011), pp. 5863-5872

[14] Shiraishi, Satomi, et al. "Knowledge-based prediction of plan quality metrics in intracranial stereotactic radiosurgery." Medical physics 42.2 (2015): 908-917.

[15] Ohira, Shingo, et al. "HyperArc VMAT planning for single and multiple brain metastases stereotactic radiosurgery: a new treatment planning approach." Radiation Oncology 13.1 (2018): 13.

[16] J. Roper, V. Chanyavanich, G. Betzel, J. Switchenko, A. Dhabaan Single-isocenter multiple-target srs: Risk of compromised coverage Int J Radiat Oncol Biol Phys, 93 (2015), pp. 540-546

[17] Faught, Austin M., et al. "Re-examining TG-142 recommendations in light of modern techniques for linear accelerator based radiosurgery." Medical physics 43.10 (2016): 5437-5441.

[18] Thomas, Andrew, et al. "A comprehensive investigation of the accuracy and reproducibility of a multitarget single isocenter VMAT radiosurgery technique." Medical physics 40.12 (2013): 121725.

[19] Adamson, Justus, et al. "Delivered Dose Distribution Visualized Directly With Onboard kV-CBCT: Proof of Principle." International Journal of Radiation Oncology* Biology* Physics 103.5 (2019): 1271-1279.

[20] Pant, Kiran, et al. "Comprehensive Radiation and Imaging Isocenter Verification Using NIPAM kV-CBCT Dosimetry." *Medical Physics* (2020).

[21] Alongi, F., Fiorentino, A., Gregucci, F. et al. J Cancer Res Clin Oncol (2019) 145: 193. https://doi.org/10.1007/s00432-018-2781-7

[22] Gregucci, Fabiana, et al. "Linac-based radiosurgery or fractionated stereotactic radiotherapy with flattening filter-free volumetric modulated arc therapy in elderly patients." Strahlentherapie und Onkologie 195.3 (2019): 218-225.

[23] Lau, Steven KM, et al. "Single-isocenter frameless volumetric modulated arc radiosurgery for multiple intracranial metastases." Neurosurgery 77.2 (2015): 233-240.

[24] Park, J. M., Wu, H. G., Kim, J. H., Carlson, J. N. K., & Kim, K. (2015). The effect of MLC speed and acceleration on the plan delivery accuracy of VMAT. British Journal of Radiology, 88(1049), 16–24. https://doi.org/10.1259/bjr.20140698

[25] Masi, L., Doro, R., Favuzza, V., Cipressi, S., & Livi, L. (2013). Impact of plan parameters on the dosimetric accuracy of volumetric modulated arc therapy. Medical Physics, 40(7). https://doi.org/10.1118/1.4810969

[26] Kang, J. , Ford, E. C., Smith, K. , Wong, J. and McNutt, T. R. (2010), A method for optimizing LINAC treatment geometry for volumetric modulated arc therapy of multiple brain metastases. Med. Phys., 37: 4146-4154. doi:10.1118/1.3455286

[27] Wu, Q., Snyder, K. C., Liu, C., Huang, Y., Zhao, B., Chetty, I. J., & Wen, N. (2016). Optimization of treatment geometry to reduce normal brain dose in radiosurgery of multiple brain metastases with single-isocenter volumetric modulated Arc therapy. *Scientific Reports*, *6*(June), 1–8. https://doi.org/10.1038/srep34511

[28] Yuan Y, Thomas EM, Clark GA, Markert JM, Fiveash JB, Popple RA. Evaluation of multiple factors affecting normal brain dose in single-isocenter multiple target radiosurgery. J Radiosurgery SBRT. 2018;5(2):131-144.

[29] Das, I. J., Cheng, C. W., Watts, R. J., Ahnesjö, A., Gibbons, J., Li, X. A., … Zhu, T. C. (2008). Accelerator beam data commissioning equipment and procedures: Report of the TG-106 of the Therapy Physics Committee of the AAPM. Medical Physics, 35(9), 4186–4215. https://doi.org/10.1118/1.2969070

[30] Vergalasova, I., Liu, H., Alonso-Basanta, M., Dong, L., Li, J., Nie, K., … Li, T. (2019). Multi-institutional dosimetric evaluation of modern day stereotactic radiosurgery (SRS) treatment options for multiple brain metastases. Frontiers in Oncology, 9(JUN), 1–12. https://doi.org/10.3389/fonc.2019.00483

[31] Charles PH, Cranmer-Sargison G, Thwaites DI, et al. A practical and theoretical definition of very small field size for radiotherapy output factor measurements. Med Phys. 2014;41(4). doi:10.1118/1.4868461

[32] Das, I. J., Ding, G. X., & Ahnesjö, A. (2008). Small fields: Nonequilibrium radiation dosimetry. Medical Physics, 35(1), 206–215. https://doi.org/10.1118/1.2815356

[33] Zhu, T. C., Bjärngard, B. E., & Shackford, H. (1995). X-ray source and the output factor. Medical Physics, 22(6), 793–798. https://doi.org/10.1118/1.597588

[34] Battista, J. J., & Munro, P. (1995). Extrafocal Radiation: A Unified Approach to the Prediction of Beam Penumbra and Output Factors for Megavoltage X-Ray Beams. Medical Physics, 22(12), 2065–2074. https://doi.org/10.1118/1.597648

[35] Graves, M. N., Thompson, A. V., & Martel, M. K. (2001). Calibration and quality assurance for rounded leaf-end MLC systems. Medical Physics, 28(11), 2227–2233. https://doi.org/10.1118/1.1413517

[36] Lin, C. Y., Shiau, A. C., Ji, J. H., Lee, C. J., Wang, T. H., Hsu, S. H., & Liang, J. A. (2018). A simple method for determining dosimetric leaf gap with cross-field dose width for rounded leaf-end multileaf collimator systems. Radiation Oncology (London, England), 13(1), 222. https://doi.org/10.1186/s13014-018-1164-1

[37] Szpala, S., Cao, F., & Kohli, K. (2014). On using the dosimetric leaf gap to model the rounded leaf ends in VMAT/RapidArc plans. Journal of Applied Clinical Medical Physics, 15(2), 67–84. https://doi.org/10.1120/jacmp.v15i2.4484

[38] Lim, S. , Kuo, L. , Happersett, L. , Lovelock, D. , Ballangrud, A. and LoSasso, T. (2016), SU-G-BRC-05: Conundrum for VMAT Cranial Multiple Lesions Treated with HD120 MLC. Med. Phys., 43: 3628-3628. doi:10.1118/1.4956895

[39] Ballangrud, Å., Kuo, L. C., Happersett, L., Lim, S. B., Beal, K., Yamada, Y., … Mechalakos, J. (2018). Institutional experience with SRS VMAT planning for multiple cranial metastases. Journal of Applied Clinical Medical Physics, 19(2), 176–183. https://doi.org/10.1002/acm2.12284

[40] Faught, Austin M., et al. "Re-examining TG-142 recommendations in light of modern techniques for linear accelerator based radiosurgery." Medical physics 43.10 (2016): 5437-5441.

[41] Stanhope, C., Chang, Z., Wang, Z., Yin, F. F., Kim, G., Salama, J. K., … Adamson, J. (2016). Physics considerations for single-isocenter, volumetric modulated arc radiosurgery for treatment of multiple intracranial targets. Practical Radiation Oncology, 6(3), 207–213. https://doi.org/10.1016/j.prro.2015.10.010

[42] Roper, J., Chanyavanich, V., Betzel, G., Switchenko, J., & Dhabaan, A. (2015). Single-Isocenter Multiple-Target Stereotactic Radiosurgery: Risk of Compromised Coverage. International Journal of Radiation Oncology Biology Physics, 93(3), 540–546. https://doi.org/10.1016/j.ijrobp.2015.07.2262

[43] J. A. Nelder, R. Mead, A Simplex Method for Function Minimization, The Computer Journal, Volume 7, Issue 4, January 1965, Pages 308–313, https://doi.org/10.1093/comjnl/7.4.308

[44] Varian Medical Systems, Inc., 3100 Hanseth Way Palo Alto, CA 94304-1038, USA

[45] Liu, H., Sintay, B., Pearman, K., Shang, Q., Hayes, L., Maurer, J., … Wiant, D. (2018). Comparison of the progressive resolution optimizer and photon optimizer in VMAT optimization for stereotactic treatments. Journal of applied clinical medical physics, 19(4), 155–162. doi:10.1002/acm2.12355

[46] Varian Medical Systems. (2017). Eclipse Photon and Electron Algorithm Reference Guide. (April), 263–348.

[47] Stanhope C, Chang Z, Wang Z, et al. Physics considerations for single-isocenter, volumetric modulated arc radiosurgery for treatment of multiple intracranial targets. Pract Radiat Oncol. 2016;6(3):207-213. doi:10.1016/j.prro.2015.10.010

[48] Morrison J, Hood R, Yin FF, Salama JK, Kirkpatrick J, Adamson J. Is a single isocenter sufficient for volumetric modulated arc therapy radiosurgery when multiple intracranial metastases are spatially dispersed? Med Dosim. 2016;41(4):285-289. doi:10.1016/j.meddos.2016.06.007

[49] Limon D, McSherry F, Herndon J, et al. Single fraction stereotactic radiosurgery for multiple brain metastases. Adv Radiat Oncol. 2017;2(4):555-563. Doi:10.1016/j.adro.2017.09.002

[50] McNiven, A.L., Sharpe, M.B. and Purdie, T.G. (2010), A new metric for assessing IMRT modulation complexity and plan deliverability. Med. Phys., 37: 505-515.doi:10.1118/1.3276775

[51] Photon, E., Algorithms, E., & Guide, R. (2014). Eclipse Photon and Electron Algorithms Reference Guide 13485.

[52] Varian Medical Systems. (2016). TrueBeam Trajectory Log File Specification. (November), 1–12.

[53] Minniti, G., Clarke, E., Lanzetta, G., Osti, M. F., Trasimeni, G., Bozzao, A., … Enrici, R. M. (2011). Stereotactic radiosurgery for brain metastases: analysis of outcome and risk of brain radionecrosis. Radiation Oncology, 6(1), 48. https://doi.org/10.1186/1748-717X-6-48

[54] Minniti, G., D'Angelillo, R. M., Scaringi, C., Trodella, L. E., Clarke, E., Matteucci, P., … Trodella, L. (2014). Fractionated stereotactic radiosurgery for patients with brain metastases. Journal of Neuro-Oncology, 117(2), 295–301. https://doi.org/10.1007/s11060-014-1388-3

[55] Lawrence, Y. R., Li, X. A., el Naqa, I., Hahn, C. A., Marks, L. B., Merchant, T. E., & Dicker, A. P. (2010). Radiation Dose-Volume Effects in the Brain. International Journal of Radiation Oncology Biology Physics,76(3SUPPL.),20–27. https://doi.org/10.1016/j.ijrobp.2009.02.091

[56] Mark J Amsbaugh, Mehran B Yusuf, Jeremy Gaskins, Anthony E Dragun, Neal Dunlap, Timothy Guan, S. W. (2016). A Dose-Volume Response Model for Brain Metastases Treated With Frameless Single-Fraction Robotic Radiosurgery. Technology in Cancer Research & Treatment, 8(4), 1–13. https://doi.org/10.1177/1533034616685025

[57] Farrukh, S., Ilyas, N., Naveed, M., Haseeb, A., Bilal, M., Najamuddin, D., & Iqbal, J. (2017). Penumbral Dose Characteristics of Physical and Virtual Wedge Profiles. International Journal of Medical Physics, Clinical Engineering and Radiation Oncology, 06(02), 216–224. https://doi.org/10.4236/ijmpcero.2017.62020

[58] Fraass B, Doppke K, Hunt M, et al. American association of physicists in medicine radiation therapy committee task group 53: Quality assurance for clinical radiotherapy treatment planning. *Med Phys*. 1998;25(10):1773-1829. doi:10.1118/1.598373

[59] Farrukh, S., Ilyas, N., Naveed, M., Haseeb, A., Bilal, M., Najamuddin, D., & Iqbal, J. (2017). Penumbral Dose Characteristics of Physical and Virtual Wedge Profiles. International Journal of Medical Physics, Clinical Engineering and Radiation Oncology, 06(02), 216–224. https://doi.org/10.4236/ijmpcero.2017.62020

[60] Yao, W., & Farr, J. B. (2015). Determining the optimal dosimetric leaf gap setting for rounded leaf-end multileaf collimator systems by simple test fields. Journal of Applied Clinical Medical Physics, 16(4), 65–77. https://doi.org/10.1120/jacmp.v16i4.5321

[61] Hirashima, H., Nakamura, M., Miyabe, Y., Uto, M., Nakamura, K., & Mizowaki, T. (2018). Monitoring of mechanical errors and their dosimetric impact throughout the course of non-coplanar continuous volumetric-modulated arc therapy. Radiation Oncology, 13(1). https://doi.org/10.1186/s13014-018-0972-7

[62] Okumura, T., Nakashima, T., Aita, M., Ochi, Y., Kawahara, D., Masuda, H., … Nagata, Y. (2016). Verification of Mechanical and Dosimetric Accuracy for Head and Neck Volumetric Modulated Arc Therapy With Jaw Tracking. International Journal of Radiation Oncology*Biology*Physics, 96(2), E638. https://doi.org/10.1016/j.ijrobp.2016.06.2226

[63] MacDonald RL, Thomas CG, Syme A. Dynamic collimator trajectory algorithm for multiple metastases dynamic conformal arc treatment planning. Med Phys. 2018;45(1):5-17. doi:10.1002/mp.12648

[64] MacDonald RL, Thomas CG, Ward L, Syme A. Intra-Arc Binary Collimation Algorithm for the Optimization of Stereotactic Radiotherapy Treatment of Multiple Metastases with Multiple Prescriptions. Medical Physics. 0(ja). doi:10.1002/mp.13224

[65] Brainlab North American Headquarters, 5 Westbrook Corporate Centersuite 1000, Westchester, IL 60154

[66] Fusella, M., Scaggion, A., Pivato, N., Rossato, M. A., Zorz, A., & Paiusco, M. (2018). Efficiently train and validate a RapidPlan model through APQM scoring. Medical Physics, 45(6), 2611–2619. https://doi.org/10.1002/mp.12896

[67] Alongi, F., Fiorentino, A., Gregucci, F., Corradini, S., Giaj-Levra, N., Romano, L., … Ruggieri, R. (2019). First experience and clinical results using a new non-coplanar mono-isocenter technique (HyperArcTM) for Linac-based VMAT radiosurgery in brain metastases. Journal of Cancer Research and Clinical Oncology, 145(1), 193–200. https://doi.org/10.1007/s00432-018-2781-7

[68] Ohira, S., Ueda, Y., Akino, Y., Hashimoto, M., Masaoka, A., Hirata, T., … Teshima, T. (2018). HyperArc VMAT planning for single and multiple brain metastases stereotactic radiosurgery: A new treatment planning approach. Radiation Oncology, 13(1), 1–9. https://doi.org/10.1186/s13014-017-0948-z